JACC: CARDIOVASCULAR IMAGING
VOL. ■, NO. ■, 2017

ISSN 1936-878X/$36.00
PUBLISHED BY ELSEVIER
http://dx.doi.org/10.1016/j.jcmg.2016.09.030

Accuracy of Noncontrast Quiescent-Interval Single-Shot Lower Extremity MR Angiography Versus CT Angiography for Diagnosis of Peripheral Artery Disease

Comparison With Digital Subtraction Angiography

Akos Varga-Szemes, MD, PhD,[a] Julian L. Wichmann, MD,[a,b] U. Joseph Schoepf, MD,[a,c] Pal Suranyi, MD, PhD,[a,c] Carlo N. De Cecco, MD, PhD,[a] Giuseppe Muscogiuri, MD,[a,d] Damiano Caruso, MD,[a,e] Ricardo T. Yamada, MD,[a] Sheldon E. Litwin, MD,[c] Christian Tesche, MD,[a,f] Taylor M. Duguay, BS,[a] Shivraman Giri, PhD,[g] Rozemarijn Vliegenthart, MD, PhD,[a,h] Thomas M. Todoran, MD[c]

ABSTRACT

OBJECTIVES This study sought to evaluate the image quality and diagnostic accuracy of noncontrast quiescent-interval single-shot (QISS) magnetic resonance angiography (MRA) versus iodine-contrast computed tomography angiography (CTA) in patients with peripheral artery disease (PAD), with invasive digital subtraction angiography (DSA) as the reference standard.

BACKGROUND QISS is a recently introduced noncontrast MRA technique. Although the diagnostic accuracy of QISS is reportedly similar to that of contrast-enhanced MRA, its performance compared with contrast-enhanced CTA, the most frequently used noninvasive modality for evaluation of PAD, is unknown.

METHODS Thirty patients (66 ± 7 years of age) with PAD underwent lower extremity CTA with third-generation dual-source dual-energy CT and 1.5-T MRA using a prototype noncontrast QISS sequence. DSA was performed within 50 days. The abdominal aorta and lower extremity run-off were imaged. Eighteen arterial segments were analyzed. Subjective image quality (3-point Likert scale) and stenosis (5-point grading) were evaluated by 2 observers and compared using the Mann–Whitney *U* and chi-square tests, respectively. Sensitivity and specificity of MRA and CTA for >50% stenosis detection were compared using the McNemar-test.

RESULTS Of 540 segments, 15 (2.8%) and 42 (7.8%) inconclusive segments were excluded from MRA and CTA analysis, respectively ($p = 0.0006$). The DSA results were available for 410 of the remaining segments. Overall subjective image quality was rated similarly with QISS-MRA (2.52 [95% confidence interval: 2.46 to 2.57]) and CTA (2.49 [95% confidence interval: 2.43 to 2.55]; $p = 0.5062$). The sensitivity and specificity of MRA for >50% stenosis were 84.9% and 97.2%, respectively, similar to those of CTA (87.3% and 95.4%, respectively). Interobserver agreement for stenosis detection was excellent for MRA ($\kappa > 0.81$) and CTA ($\kappa > 0.81$).

CONCLUSIONS Noncontrast QISS-MRA provides high diagnostic accuracy compared with DSA, while being less prone to image artifacts than CTA. QISS better visualizes heavily calcified segments with impaired flow. QISS-MRA obviates the need for contrast administration in PAD patients. (J Am Coll Cardiol Img 2017;■:■–■) © 2017 by the American College of Cardiology Foundation.

ABBREVIATIONS AND ACRONYMS

CTA = computed tomography angiography

DSA = digital subtraction angiography

ICC = intraclass correlation coefficient

MRA = magnetic resonance angiography

PAD = peripheral artery disease

QISS = quiescent-interval single-shot

Peripheral artery disease (PAD) affects 12% to 14% of the general population and its prevalence has been shown to increase with age (1). Although segmental Doppler pressures and pulse volume recordings are appropriate techniques for evaluating symptomatic patients, more sophisticated noninvasive imaging techniques may be necessary for further anatomic delineation and treatment planning, especially before revascularization (2,3). Both computed tomography angiography (CTA) and magnetic resonance angiography (MRA) are rated as "usually appropriate" diagnostic approaches for claudication with suspected vascular etiology (2,4). Patients with PAD frequently experience several comorbidities, including renal insufficiency, which often increases concern regarding the administration of either iodinated or gadolinium-based contrast media in view of contrast-induced nephropathy and nephrogenic systemic fibrosis (5,6).

Collectively, concerns about the administration of contrast media and recent technical advances have led to an increased interest in noncontrast MRA techniques. Although many approaches to noncontrast MRA have been evaluated (7), most have limited clinical utility in patients with PAD due to either technical limitations or overestimation of mild to moderate stenoses (8,9).

Quiescent-interval single-shot (QISS) MRA is a recently introduced, robust noncontrast MRA technique (10). QISS-MRA at 1.5-T and 3-T has shown promising results with reported diagnostic accuracies being close or equal to those of contrast-enhanced MRA (11–15).

In this study, we evaluated the image quality and diagnostic accuracy of noncontrast QISS-MRA in patients with PAD against invasive digital subtraction angiography (DSA) as the reference standard and compared the results to those obtained by contrast-enhanced CTA.

MATERIALS AND METHODS

PATIENT SELECTION. Our Institutional Review Board approved the study protocol, and written informed consent was obtained from all patients. The study was conducted in compliance with the Health Insurance Portability and Accountability Act of 1996 guidelines. Thirty patients were enrolled prospectively at our institution between May 2014 and June 2015. All patients were referred for a clinically indicated lower extremity runoff CTA for the evaluation of known or suspected PAD as a preparatory procedure for revascularization. General magnetic resonance imaging exclusion criteria were applied to patient selection. The MRA and CTA were scheduled as consecutive procedures no more than 50 days before the invasive angiography study.

QISS NONCONTRAST MRA ACQUISITION PROTOCOL. All patients underwent magnetic resonance imaging as the study procedure on a 1.5-T magnetic resonance imaging scanner (MAGNETOM Avanto, Siemens Healthineers, Erlangen, Germany) using phased-array radiofrequency body, peripheral and spine matrix coils with 2×6 body elements positioned anteriorly on the abdomen and pelvis, 36 elements positioned anteriorly on the lower extremities, and 32 elements positioned posteriorly. Imaging was performed in a free-breathing fashion except in the abdominal stations, with the patient in a feet-first supine position. QISS-MRA was performed using an investigational prototype sequence without applying scout imaging. Image acquisition was carried out under electrocardiographic gating starting from the feet to the abdomen according to a previously described protocol (10). The entire abdominal aorta and lower extremity runoff were covered by 8 to 9 groups of 48 sections that were 3 mm thick ("stations"), with each station covering a 144-mm *z*-axis volume. The following additional acquisition parameters were used: field of

From the [a]Division of Cardiovascular Imaging, Department of Radiology and Radiological Science, Medical University of South Carolina, Charleston, South Carolina; [b]Department of Diagnostic and Interventional Radiology, University Hospital Frankfurt, Frankfurt, Germany; [c]Division of Cardiology, Department of Medicine, Medical University of South Carolina, Charleston, South Carolina; [d]Department of Medical-Surgical Sciences and Translational Medicine, University of Rome "Sapienza," Rome, Italy; [e]Department of Radiological, Oncological and Pathological Sciences, University of Rome "Sapienza," Rome, Italy; [f]Department of Cardiology and Intensive Care Medicine, Heart Center Munich-Bogenhausen, Munich, Germany; [g]Siemens Medical Solutions, Chicago, Illinois; and the [h]University of Groningen, University Medical Center Groningen, Center for Medical Imaging-North East Netherlands, Department of Radiology, Groningen, the Netherlands. Drs. Varga-Szemes and De Cecco have received consulting fee from Guerbet and Siemens. Dr. Schoepf is a consultant for Guerbet; and has received research grants from Astellas, Bayer, Bracco, GE Healthcare, Medrad, and Siemens Healthineers. Dr. Giri is an employee of Siemens. All other authors have reported that they have no relationships relevant to the contents of this paper to disclose.

Manuscript received March 11, 2016; revised manuscript received September 26, 2016, accepted September 29, 2016.

view, 400 × 260 mm^2; measured voxel size, 1 × 1 × 3 mm^3; reconstructed voxel size, 0.5 × 0.5 × 3 mm^3; repetition time, 3.5 ms; echo time, 1.4 ms; flip angle, 90°; bandwidth, 658 Hz/pixel; quiescent interval, 226 ms; a generalized autocalibrating partially parallel acquisition with an acceleration factor of 2, and Cartesian readout were applied. Acquisition time and door-to-door time were recorded.

CONTRAST-ENHANCED CTA ACQUISITION PROTOCOL AND IMAGE RECONSTRUCTION. The CTA image acquisition was performed on a third generation dual-source CT system (Somatom Definition Force, Siemens Healthineers, Forchheim, Germany) in dual-energy mode (16). Acquisitions covered the region from the distal abdominal aorta down to the toes and included a topogram and a noncontrast scan followed by a contrasted angiogram.

Iodinated contrast material (350 mgI/ml iohexol, Omnipaque, GE Healthcare, Chalfont St. Giles, United Kingdom) was administered intravenously with a multiphasic injection using an automated dual-syringe power injector (Stellant D CT Injection System, Medrad, Inc., Warrendale, Pennsylvania) according to the protocol described by Fleischmann et al. (17). A 120-kV bolus tracking approach (CareBolus, Siemens) with a threshold of 115 Hounsfield units applied in the abdominal aorta was used to time the scan initiation. Acquisition was performed using the following parameters: field of view, 350 mm; pitch 0.7; collimation, 2 × 64 × 0.6 mm for both detectors; and tube voltage and current, 150 kV/59 reference mAs for tube A and 90 kV/95 reference mAs for tube B. Acquisition time and door-to-door time were recorded. The latter included the time needed for contrast material loading, injector preparation, and patient instructions. Datasets were reconstructed using a soft tissue convolution kernel (Qr40, Siemens) with a section thickness and increment of 1.5 mm and 1.0 mm, respectively. Third generation advanced modeled iterative reconstruction algorithm (ADMIRE, Siemens) at a strength level of 3 was used (18). For further analysis, images were reconstructed using a noise-optimized virtual monochromatic imaging algorithm at 50 keV on a dedicated workstation (syngo.via, Siemens) (16).

DSA PROTOCOL. Patients underwent invasive DSA as a standard of care procedure, which was used as the reference modality in our investigation. The performing operator was aware of the initial clinical CTA results which were used for DSA procedure planning. DSA was performed by an experienced interventional cardiologist via the transfemoral approach using a cardiovascular imaging system (Axiom Artis, Siemens). A 5-F Omni Flush catheter (Angiodynamics, Queensbury, New York) was used to deliver contrast media. The tip of the catheter was positioned above the aortic bifurcation and 80 ml of nonionic iodinated contrast media (350 mgI/ml iohexal, Omnipaque, or 320 mgI/ml iodixanol, Visipaque, GE Healthcare, chosen at the discretion of the cardiologist) was injected. Pelvic and lower extremity arteries were imaged using the stepping table DSA technique in a posteroanterior projection. At the level of the iliac and common femoral arteries, additional 30° left and 30° right anterior oblique projections were obtained. Patients were treated at the time of diagnostic DSA imaging. In a few patients, DSA was only performed in 1 lower extremity (as clinically deemed necessary).

IMAGE ANALYSIS. Two independent experienced observers performed image assessments of QISS-MRA and CTA. The observers performed the image quality ratings and stenosis detection and grading independent of each other. The observers first evaluated all QISS-MRA datasets in random order. After an interval of 14 days (to minimize recall), the observers performed the assessment of CTA images, also in random order. In cases of disagreement, a third expert imager arbitrated. The QISS-MRA and CTA datasets were evaluated on dedicated workstations (Leonardo, Siemens and syngo.via VA30, Siemens, respectively). Multiplanar reconstruction and coronal maximum intensity projection images (at 20 mm thickness for both QISS-MRA and CTA) were generated from the entire axial dataset. However, axial datasets were also available to the readers. DSA cine images were reviewed on a picture archive and communication system (IMPAX 6.5, AGFA Healthcare, Ghent, Belgium) by the interventional cardiologist.

Image evaluation was performed on a per-segment basis according to an 18-segment model (19). The overall image quality was rated subjectively independently by both observers according to a 3-point grading system: 1) vascular segment not assessable due to severe image artifacts and/or poor vascular signal, resulting in low reader confidence; 2) acceptable image quality with minor artifacts and/or moderately homogenous vascular signal, resulting in marginal reader confidence; or 3) excellent image quality without artifacts and homogenous vascular signal, providing high reader confidence. Quality scores 2 and 3 were considered acceptable for diagnostic purposes.

Vessel segment stenoses were graded using a 5-point grading scale as follows: 1 (normal), 2 (mild, <50% diameter stenosis); 3 (moderate, 50% to 74%), 4 (severe, 75% to 99%), and 5 (total occlusion).

Grades 1 and 2 were considered insignificant, whereas grades 3 to 5 were interpreted as significant for diagnostic accuracy testing. In case of concurrent arterial stenoses in a single arterial segment, only the stenosis with the higher grade was evaluated.

STATISTICAL ANALYSIS. Statistical analyses were performed using MedCalc version 13.2.2 (MedCalc Software, Ostend, Belgium). The Kolmogorov-Smirnov test was used to assess normal distribution of the continuous data. Continuous variables were reported as mean ± SD, and categorical variables as absolute frequencies and proportions. The difference in acquisition time and door-to-door time was assessed using 2-tailed paired samples Student *t* test. The frequency of the different image artifacts was compared between MRA and CTA using the Mann-Whitney *U* test.

Differences in subjective image quality were assessed by averaging the 3-point score provided by the 2 observers and then comparing QISS-MRA and CTA by using the Mann-Whitney *U* test. Agreement regarding the subjective image quality ratings was assessed using intraclass correlation coefficients (ICC) with the level of agreement as follows: poor, ICC $<$ 0.20; fair, ICC $=$ 0.21 to 0.40; moderate, ICC $=$ 0.41 to 0.60; good, ICC $=$ 0.61 to 0.80; and excellent, ICC $>$ 0.80. The ICC results were reported with 95% confidence intervals (CI) in square brackets.

Differences in significant stenosis detection rate of QISS-MRA and CTA were analyzed with a chi-square test and correlation between the 2 techniques was evaluated using ICC with the level of agreement as described. Sensitivity and specificity were calculated on a per-segment basis. Agreement regarding the detection of stenosis between observers was assessed using Kappa-statistics with the level of agreement as follows: poor, $\kappa < 0.20$; fair, $\kappa = 0.21$ to 0.40; moderate, $\kappa = 0.41$ to 0.60; good, $\kappa = 0.61$ to 0.80; and excellent, $\kappa > 0.80$. The κ values were reported with 95% (CI) in square brackets. Values of $p < 0.05$ were considered significant.

RESULTS

Our study population consisted of 30 patients (mean age 66 ± 7 years; range 52 to 81 years), including 16 men (mean age 66 ± 7 years; range 55 to 81 years) and 14 women (mean age 67 ± 7 years; range 52 to 79 years). Indications for imaging were evaluation of vascular status because of intermittent claudication (n = 29) and rest pain (n = 1) for procedure planning before revascularization. The mean patient body weight and body mass index were 81.9 ± 22.4 kg (range 42.2 to 125.0 kg) and 28.2 ± 7.0 kg/m^2 (range 16.0 to 45.0 kg/m^2), respectively. Further characteristics of the patient population are detailed in Table 1, and representative clinical cases are shown in Figure 1.

TABLE 1 Patient Characteristics (n = 30)

Age, yrs	66 ± 7
Male	16 (53.3)
Race	
African American	11 (36.6)
Caucasian	19 (63.3)
Weight, kg	81.9 ± 22.4
Height, cm	170.0 ± 9.7
Body mass index, kg/m^2	28.2 ± 7.0
Diabetes mellitus	14 (46.6)
Hypertension	26 (86.6)
Dyslipidemia	26 (86.6)
Reduced renal function	
eGFR <30 ml/min/1.73 m^2	3 (10)
eGFR 30–44 ml/min/1.73 m^2	6 (20)
Smoking	
Current	8 (26.6)
Previous	17 (56.6)
Fontaine classification	
IIa	6 (20)
IIb	23 (76.6)
III	1 (3.3)
Lower leg stent	8 (26.7)
Known coronary artery disease	21 (70)
Prior myocardial infarction	7 (23.3)
Prior transient ischemic attack	4 (13.3)
Prior percutaneous coronary intervention	15 (50)
Prior coronary artery bypass surgery	10 (33.3)

Values are mean ± SD or n (%).
eGFR = estimated glomerular filtration rate.

The average acquisition time of QISS-MRA from the start of the first acquisition to the end of the entire session was 21.6 ± 3.6 min (range 16 to 29 min), including the time needed when certain stations had to be repeated. The door-to-door time was approximately 4 min longer (25.6 ± 3.3 min). The average CTA acquisition time from the start of the topogram to the end of the scanning session including pauses in between acquisitions was 4.1 ± 1.0 min ($p < 0.0001$ compared with QISS-MRA), ranging from 3.1 to 5.4 min. The CTA door-to-door time was 11.3 ± 2.1 min ($p = 0.0001$ compared with QISS-MRA). When accounting for the time required for CTA patient preparation (e.g., intravenous access insertion, point-of-care creatinine measurements before contrast media administration), the total time increased to 24.4 ± 2.7 min ($p = 0.0936$ compared with QISS-MRA door-to-door time).

A total of 540 vascular segments were imaged by QISS-MRA and CTA. Overall subjective image quality

FIGURE 1 Representative Case Examples

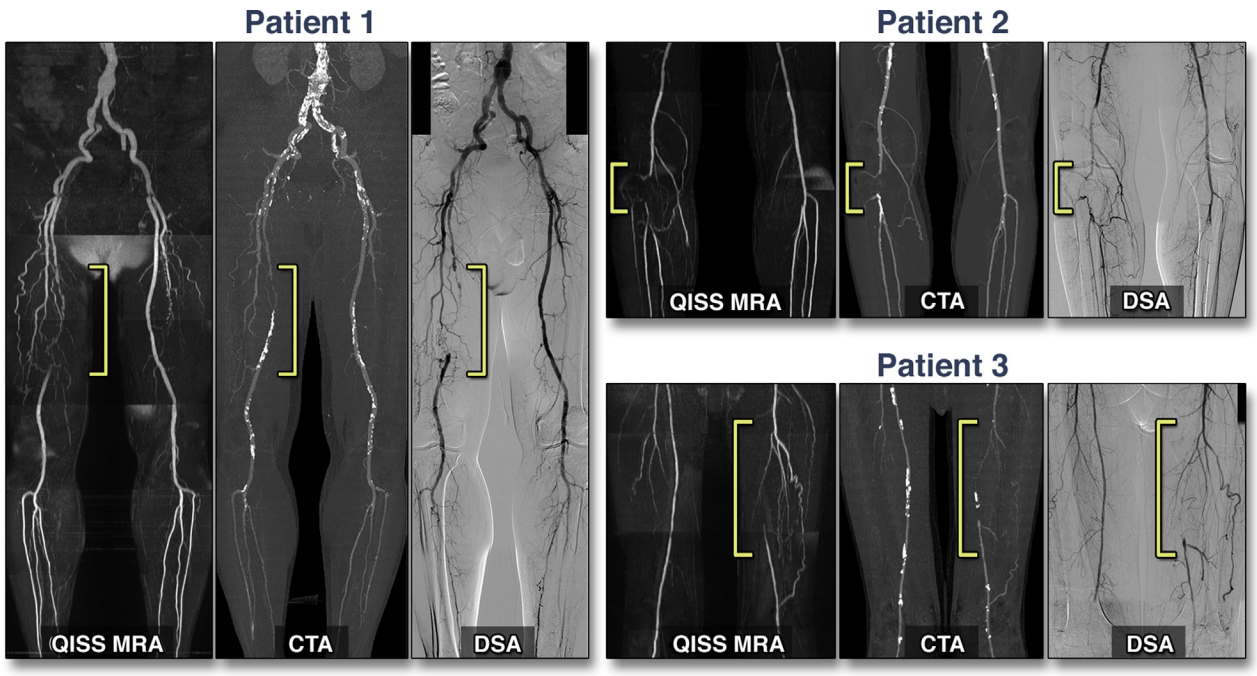

Corresponding quiescent-interval single-shot magnetic resonance angiography (QISS-MRA), computed tomography angiography (CTA), and digital subtraction angiography (DSA) images in 3 different patients with peripheral artery disease (PAD). Patient #1 is a 75-year-old man with complete occlusion of the right superficial femoral artery **(brackets)**. Although the massive calcification limits the evaluation of luminal stenosis with CTA, QISS-MRA provides close to identical angiographic assessment compared with DSA. Patient #2 is a 71-year-old man with right infrapopliteal occlusion **(brackets)** and subsequent extensive collateral circulation visualized by all 3 techniques. Patient #3 is a 63-year-old man with proximal occlusion of the left superficial femoral artery reconstituting distally via collaterals from the profunda femoral artery **(brackets)**.

was rated similarly with QISS-MRA (2.52 [95% CI: 2.46 to 2.57]) and CTA (2.49 [95% CI: 2.43 to 2.55]; p = 0.5062). Interobserver agreement in QISS-MRA and CTA ratings was good to excellent for the assessment of overall subjective image quality (ICC 0.79 [95% CI: 0.77 to 0.81] and 0.82 [95% CI: 0.78 to 0.86], respectively).

On the basis of the image quality ratings, 15 segments (2.8%) were deemed nondiagnostic (i.e., receiving score of 1 for image quality assessment) and thus were excluded from the QISS-MRA accuracy analysis for the following reasons: stent artifacts (n = 8; 1.4%), signal loss due to heavy calcification (n = 1; 0.2%), and other image artifacts including motion and radiofrequency noise artifacts (n = 6; 1.1%). Forty-two segments (7.8%; p = 0.0006 compared with QISS-MRA) were considered nondiagnostic and excluded from the CTA accuracy analysis due to stent artifacts (n = 11 [2%]; p = 0.4985 compared with QISS-MRA), heavy calcification (n = 8 [1.4%]; p = 0.0262 compared with QISS-MRA), and suboptimal opacification (n = 23; 4.3%). Representative cases with nondiagnostic segments are shown in Figures 2 and 3.

Reference DSA data were available for 410 of the remaining segments, in which the MRA and CTA images had been deemed diagnostic. The frequency of the different stenosis severity grades based on DSA, QISS-MRA, and CTA are shown in Table 2. Stenosis severity in segments with mild stenosis was overestimated in 8 (1.9%) and 13 (3.1%) segments, respectively, compared with DSA. In segments with moderate stenosis, stenosis severity was underestimated in 19 (4.6%) and 16 (3.9%) segments based on QISS-MRA and CTA, respectively. Of the 410 segments, >50% stenosis was detected by QISS-MRA, CTA, and DSA in 115 (28.0%; 8 false-positive results), 123 (30%; 13 false-positive results), and 126 (30.7%) segments, respectively. No difference between the stenosis detection rates of QISS-MRA and CTA was observed (p = 0.2561). The ICC analysis showed good agreement between QISS-MRA and CTA (0.77 [95% CI: 0.73 to 0.81]). Of the 410 segments,

FIGURE 2 Stent Artifacts

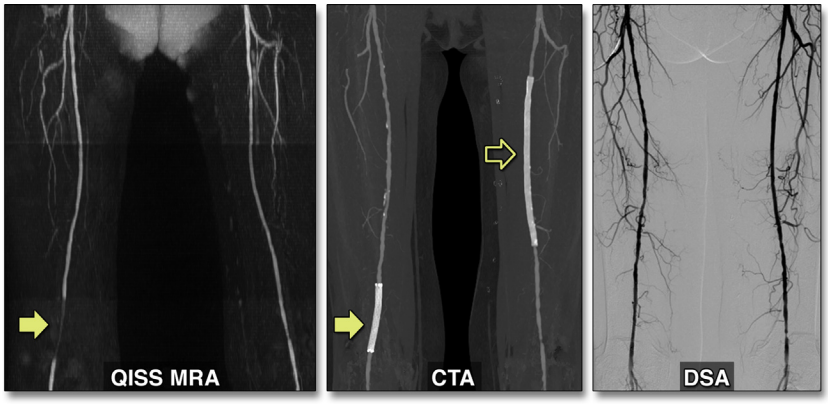

Corresponding QISS-MRA, CTA, and DSA images from a 71-year-old woman with stents in the right **(solid arrow)** and left **(open arrow)** superficial femoral arteries. Both self-expanding stents are made of nitinol (nickel-titanium alloy) and are patent on DSA. However, the stents' architecture is different, which may explain why the stent in the right superficial femoral artery causes significant signal loss in QISS MRA, whereas the visualization of the vascular lumen was not affected in the left superficial femoral artery. Abbreviations as in Figure 1.

disagreement between QISS-MRA and CTA was observed in 29 segments (7.0%). There were 18 segments (4.3%) in which CTA showed significant stenosis whereas QISS-MRA was interpreted as normal or nonsignificant stenosis. In contrast, there were 11 segments (2.6%) considered positive by QISS-MRA and negative by CTA. The sensitivity and specificity for the detection of >50% stenosis by the QISS-MRA and CTA techniques are shown in Table 3.

Interobserver agreement regarding the detection of >50% stenosis was excellent for the QISS-MRA ($\kappa = 0.84$ [95% CI: 0.82, 0.86]) and CTA ($\kappa = 0.81$ [95% CI: 0.80, 0.82]) approaches.

DISCUSSION

This prospective study of patients with PAD investigated the diagnostic accuracy of noncontrast QISS-MRA versus contrast-enhanced CTA for the detection of lower extremity vascular stenosis in one of the largest DSA-correlated cohorts to date. On a per-segment analysis, QISS-MRA showed high sensitivity and specificity, and the detection rate of >50% stenosis based on QISS-MRA was similar to that of CTA. Such an accurate noncontrast MRA approach has particular benefits in the pre-procedural diagnostic workup of PAD patients with an elevated medical risk profile.

The acquisition time measured during the QISS-MRA sessions in this study was comparable to the scan time reported by others (20). The acquisition and door-to-door times of QISS-MRA are longer than those of CTA due to the differing technological bases of these approaches. However, the time spent with each patient may be shorter for a noncontrast MRA procedure due to the additional preparation that is needed for CTA.

Image quality was rated subjectively by 2 experienced observers in this study, and QISS-MRA was found to provide similar subjective vascular signal to that of CTA. The major factors contributing to insufficient vascular delineation and increased image noise that rendered a segment nondiagnostic in QISS-MRA were the presence of certain types of stents, and radiofrequency noise. Although stent artifacts are difficult to eliminate, newly developed sequence versions with fast low-angle shot or ultrashort echo readout show better performance in patients with metallic implants, and may also be promising for vascular segments with stents (21,22). In the CTA datasets, the major source of nondiagnostic segments was the presence of stents, heavy calcification, and suboptimal opacification. The latter contributed to the exclusion of 4.3% of the segments. Of the 8 segments excluded from CTA due to heavy calcification, 7 were diagnostic with QISS-MRA. Moreover, the 23 segments excluded from CTA due to insufficient opacification were visualized with diagnostic quality by QISS-MRA. Although extreme calcification may cause signal loss in QISS-MRA, it is less affected by this artifact type compared with CTA. Suboptimal opacification is

caused by the undesirable scenario that the scanner "outruns" the slow contrast bolus. This is due to the reduced flow in severely atherosclerotic vessels and is observed in the calf arteries in most cases. As emphasized by the American College of Radiology guidelines, the 2 major shortcomings limiting image interpretation of CTA in patients with PAD are the relatively difficult acquisition timing after contrast administration due to reduced flow in the stenotic vessels and reduced lumen visibility due to heavily calcified atheromatous lesions (2). As we have shown, QISS-MRA is able to overcome both of these limitations and provides reliable findings when compared with invasive DSA.

Stenosis grading based on QISS-MRA showed good agreement with DSA. Nearly 90% of the segments were graded properly by QISS-MRA, similar to CTA, indicating that QISS-MRA can potentially be used for stenosis severity assessment. The diagnostic accuracy of noncontrast QISS-MRA evaluated here against DSA showed a sensitivity and specificity of 85% and 97%, respectively. These results are in agreement with accuracy data reported by others (20), or slightly lower compared with studies using noninvasive contrast-enhanced MRA as a reference standard (12,14). As shown here, the specificity of QISS-MRA for arterial stenosis in the lower extremities is very high, and demonstrates superiority compared with, for example, subtracted 3-dimensional fast spin echo MRA (23). Although the majority of initial QISS-MRA studies were performed at the more widely available 1.5-T field strength (10–13), QISS-MRA has also shown good diagnostic accuracy at higher field strengths (15,20,24,25).

The QISS-MRA technique was first introduced in 2010 by Edelman et al. (10). This electrocardiographic-triggered technique uses initial saturation pulses followed by 2-dimensional single-shot balanced steady-state free precession readout with a quiescent interval between them. Two saturation pulses are used, one to suppress the background signal and one applied inferior to the slice to suppress the venous blood signal. The quiescent interval before the readout allows the inflow of unsaturated arterial spins into the imaging plane. Due to its design, the flow sensitivity of QISS-MRA is negligible compared with other noncontrast techniques, such as time of flight, 3-dimensional fast spin echo-based approaches, and ungated ghost MRA (11). Additionally, single-shot 2-dimensional balanced steady-state free precession acquisition makes this technique relatively insensitive to patient motion.

Novel technological innovations in development promise to facilitate further the clinical implementation of QISS-MRA. QISS-MRA can be performed without electrocardiographic gating by using prospective self-navigation based on the detection of the acceleration of blood flow during systole with a reference-less phase contrast navigator

FIGURE 3 Benefits of QISS-MRA Over CTA

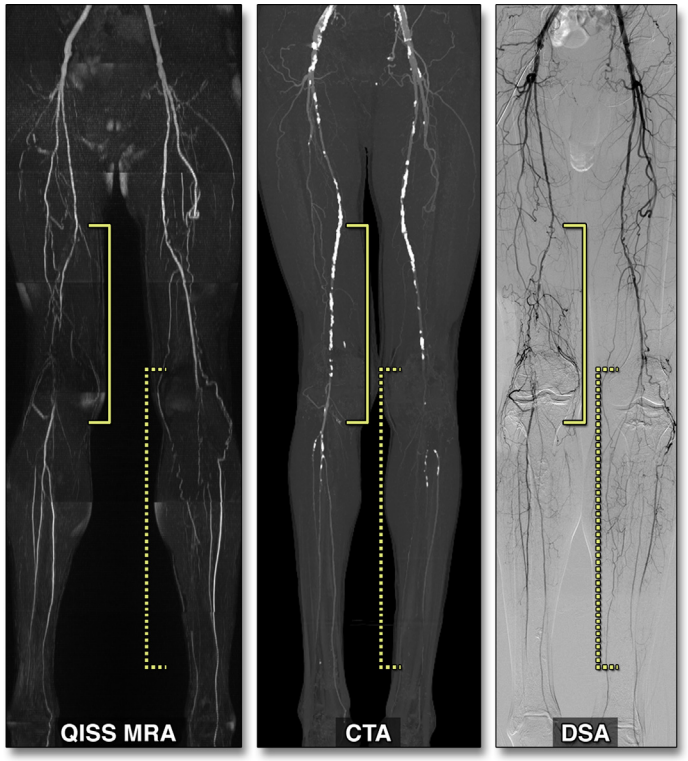

Corresponding QISS-MRA, CTA, and DSA images in a 65-year-old man. Complete lumen visualization with CTA was limited due to the presence of heavy calcification, especially in the right superficial femoral artery **(solid brackets)**. Consequently, the length of the occlusion could not be determined. However, QISS-MRA was able to visualize sufficiently the heavily calcified segments as well. The evaluation of the left calf vessels by CTA was inconclusive due to suboptimal opacification caused by the slower flow in the stenotic arteries **(dotted brackets)**. However, the reduced flow rate in the calf arteries did not affect vascular delineation in QISS-MRA. Abbreviations as in Figure 1.

TABLE 2 Frequency of Different Stenosis Severity Grades (n = 410)

Grade	DSA	QISS-MRA	CTA
1, Normal	208 (50.7)	215 (52.4)	201 (49.0)
2, Mild	76 (18.5)	80 (19.5)	86 (20.9)
3, Moderate	79 (19.2)	70 (17.0)	69 (16.8)
4, Severe	37 (9.0)	35 (8.5)	44 (10.7)
5, Total occlusion	10 (2.4)	10 (2.4)	10 (2.4)

Values are n (%).

CTA = computed tomography angiography; DSA = digital subtraction angiography; QISS-MRA = quiescent interval single-shot magnetic resonance angiography.

TABLE 3 Per-Segment Test Characteristics of QISS-MRA and CTA for the Detection of Hemodynamically Significant (>50%) Stenosis in the Lower Extremity Arteries Compared With DSA

	Sensitivity (%)	95% CI	Specificity (%)	95% CI
QISS-MRA	84.9 (107/126)	77.5-90.7	97.2 (276/284)	94.5-98.8
CTA	87.3 (110/126)	80.2-92.6	95.4 (271/284)	92.3-97.5

Values are % (n/N).
CI = confidence interval; other abbreviations as in Table 2.

(26). Highly undersampled radial k-space readout enables the acquisition of multiple 2-dimensional slices in a single cardiac cycle, which shortens the acquisition time of a complete lower extremity runoff MRA to about 2 min (27). High-resolution QISS-MRA provides 1.5-mm section thickness and thus a more detailed visualization of the vascular anatomy (28). Quiescent interval low-angle shot MRA provides superior image quality for the external carotid arteries compared with 2-dimensional time of flight with an average acquisition time of <6 min (29). As discussed, QISS-MRA is a rapidly developing technology with significant clinical potential. Recently, QISS-MRA has been released as a product and is available for clinical care.

STUDY LIMITATIONS. Our patient population was enrolled from a single university medical center. Further multicenter studies may be necessary to confirm the diagnostic performance of QISS-MRA across a wider range of patients, indications, and clinical scenarios. Although the maximum time interval between QISS-MRA and DSA was kept as short as feasible in our study, disease progression during this time period could have occurred. In this investigation, we did not include a comparison with contrast enhanced MRA to gauge the performance of our proposed noncontrast technique, because this strategy has been used before and DSA as a stronger reference standard was available. We did not perform an objective image quality analysis due to the differing physical nature of the various imaging tests. Moreover, the QISS sequence involves parallel imaging, which makes the calculation of objective image quality measures unsuitable (30). For valid signal-to-noise and contrast-to-noise ratio measurements, acquisitions would have to be repeated at least 3 times, which would have increased the acquisition time unreasonably. Although dual-energy based calcium removal was attempted to improve lumen visualization with CTA, calcium removal caused the apparent disruption of vessel continuity in several cases where DSA clearly indicated intact flow. As a result, we chose not to use calcium removal in the final CTA image analysis.

CONCLUSIONS

This study indicates that noncontrast QISS-MRA provides high diagnostic accuracy for the detection of arterial stenosis of the lower extremities at 1.5-T. QISS-MRA is a feasible alternative for patients with contraindications to contrast media, especially in light of recently released professional guidelines that widened the population considered at risk for nephrogenic systemic fibrosis to patients with estimated glomerular filtration rate of <40 ml/min/1.73 m^2 (31). Furthermore, QISS-MRA may avoid the timing-related difficulties of contrast-enhanced CTA and result in better visualization of heavily calcified arteries.

REPRINT REQUESTS AND CORRESPONDENCE: Dr. U. Joseph Schoepf, Division of Cardiovascular Imaging, Department of Radiology and Radiological Science, Medical University of South Carolina, Ashley River Tower, 25 Courtenay Drive, MSC 226, Charleston, South Carolina 29425-2260. E-mail: schoepf@musc.edu.

PERSPECTIVES

COMPETENCY IN MEDICAL KNOWLEDGE: In patients with PAD, noncontrast QISS-MRA identifies significant arterial stenosis with 85% sensitivity and 97% specificity, providing similar diagnostic accuracy to that of CTA. QISS-MRA shows superior performance to CTA in that it visualizes vascular segments with extensive intraluminal calcification better, and, being a noncontrast technique, its intravascular signal quality is not influenced by timing after contrast administration. Furthermore, QISS-MRA provides excellent interobserver agreement, highly rated subjective image quality, and comparable patient care time.

TRANSLATIONAL OUTLOOK: Additional multicenter, prospective studies are needed to show that QISS-MRA, a noncontrast noninvasive imaging technique, provides high diagnostic confidence and diagnostic accuracy for the detection of significant lower extremity arterial stenosis. Additionally, QISS needs to be tested in other organ systems as well, to understand fully its potential applications. Such studies may establish ultimately its clinical usefulness in vascular imaging of patients in whom kidney disease or other contraindications would prevent CT or magnetic resonance contrast material administration.

REFERENCES

1. Hiatt WR, Hoag S, Hamman RF. Effect of diagnostic criteria on the prevalence of peripheral arterial disease. The San Luis Valley Diabetes Study. Circulation 1995;91:1472–9.

2. Expert Panel on Vascular Imaging, Dill KE, Rybicki FJ, et al. American College of Radiology Appropriateness Criteria® Claudication - Suspected Vascular Etiology. Available at: https://acsearch.acr.org/docs/69411/Narrative/. Accessed February 15, 2016.

3. Norgren L, Hiatt WR, Dormandy JA, et al. Inter-society consensus for the management of peripheral arterial disease. Int Angiol 2007;26:81–157.

4. Rooke TW, Hirsch AT, Misra S, et al. Management of patients with peripheral artery disease (compilation of 2005 and 2011 ACCF/AHA Guideline Recommendations): a report of the American College of Cardiology Foundation/American Heart Association Task Force on Practice Guidelines. J Am Coll Cardiol 2013;61:1555–70.

5. Davenport MS, Khalatbari S, Cohan RH, Dillman JR, Myles JD, Ellis JH. Contrast material-induced nephrotoxicity and intravenous low-osmolality iodinated contrast material: risk stratification by using estimated glomerular filtration rate. Radiology 2013;268:719–28.

6. Kuo PH, Kanal E, Abu-Alfa AK, Cowper SE. Gadolinium-based MR contrast agents and nephrogenic systemic fibrosis. Radiology 2007;242:647–9.

7. Miyazaki M, Lee VS. Nonenhanced MR angiography. Radiology 2008;248:20–43.

8. Lim RP, Hecht EM, Xu J, et al. 3D nongadolinium-enhanced ECG-gated MRA of the distal lower extremities: preliminary clinical experience. J Magn Reson Imaging 2008;28:181–9.

9. Haneder S, Attenberger UI, Riffel P, Henzler T, Schoenberg SO, Michaely HJ. Magnetic resonance angiography (MRA) of the calf station at 3.0 T: intraindividual comparison of non-enhanced ECG-gated flow-dependent MRA, continuous table movement MRA and time-resolved MRA. Eur Radiol 2011;21:1452–61.

10. Edelman RR, Sheehan JJ, Dunkle E, Schindler N, Carr J, Koktzoglou I. Quiescent-interval single-shot unenhanced magnetic resonance angiography of peripheral vascular disease: Technical considerations and clinical feasibility. Magn Reson Med 2010;63:951–8.

11. Offerman EJ, Hodnett PA, Edelman RR, Koktzoglou I. Nonenhanced methods for lower-extremity MRA: a phantom study examining the effects of stenosis and pathologic flow waveforms at 1.5T. J Magn Reson Imaging 2011;33:401–8.

12. Hodnett PA, Koktzoglou I, Davarpanah AH, et al. Evaluation of peripheral arterial disease with nonenhanced quiescent-interval single-shot MR angiography. Radiology 2011;260:282–93.

13. Hodnett PA, Ward EV, Davarpanah AH, et al. Peripheral arterial disease in a symptomatic diabetic population: prospective comparison of rapid unenhanced MR angiography (MRA) with contrast-enhanced MRA. AJR Am J Roentgenol 2011;197:1466–73.

14. Klasen J, Blondin D, Schmitt P, et al. Non-enhanced ECG-gated quiescent-interval single-shot MRA (QISS-MRA) of the lower extremities: comparison with contrast-enhanced MRA. Clin Radiol 2012;67:441–6.

15. Hansmann J, Morelli JN, Michaely HJ, et al. Nonenhanced ECG-gated quiescent-interval single shot MRA: Image quality and stenosis assessment at 3 tesla compared with contrast-enhanced MRA and digital subtraction angiography. J Magn Reson Imaging 2014;39:1486–93.

16. Wichmann JL, Gillott MR, De Cecco CN, et al. Dual-energy computed tomography angiography of the lower extremity runoff: impact of noise-optimized virtual monochromatic imaging on image quality and diagnostic accuracy. Invest Radiol 2016;51:139–46.

17. Fleischmann D, Kamaya A. Optimal vascular and parenchymal contrast enhancement: the current state of the art. Radiol Clin North Am 2009;47:13–26.

18. Solomon J, Mileto A, Ramirez-Giraldo JC, Samei E. Diagnostic performance of an advanced modeled iterative reconstruction algorithm for low-contrast detectability with a third-generation dual-source multidetector CT Scanner: potential for radiation dose reduction in a multireader study. Radiology 2015;275:735–45.

19. Fraioli F, Catalano C, Napoli A, et al. Low-dose multidetector-row CT angiography of the infrarenal aorta and lower extremity vessels: image quality and diagnostic accuracy in comparison with standard DSA. Eur Radiol 2006;16:137–46.

20. Wagner M, Knobloch G, Gielen M, et al. Non-enhanced peripheral MR-angiography (MRA) at 3 Tesla: evaluation of quiescent-interval single-shot MRA in patients undergoing digital subtraction angiography. Int J Cardiovasc Imaging 2015;31:841–50.

21. Edelman RR, Giri S, Murphy IG, O'Brien K, Robson MD, Koktzoglou I. QISS UTE: quiescent-inflow single-shot MRA of the peripheral arteries using an ultra-short echo time readout. International Society for Magnetic Resonance in Medicine 23rd Annual Meeting and Exhibition, May 30–June 5, 2015; Toronto, Canada (abstract).

22. Murphy IG, Koktzoglou I, Giri S, Edelman RR, Botelho MP. Reduction in metal susceptibility artifact from hip prostheses using QISS with fast low angle shot readout. Radiological Society of North America 2015 Scientific Assembly and Annual Meeting, November 29–December 4, 2015; Chicago, IL (abstract).

23. Ward EV, Galizia MS, Usman A, Popescu AR, Dunkle E, Edelman RR. Comparison of quiescent inflow single-shot and native space for non-enhanced peripheral MR angiography. J Magn Reson Imaging 2013;38:1531–8.

24. Knobloch G, Gielen M, Lauff MT, et al. ECG-gated quiescent-interval single-shot MR angiography of the lower extremities: initial experience at 3 T. Clin Radiol 2014;69:485–91.

25. Amin P, Collins JD, Koktzoglou I, et al. Evaluating peripheral arterial disease with unenhanced quiescent-interval single-shot MR angiography at 3 T. AJR Am J Roentgenol 2014;202:886–93.

26. Offerman EJ, Koktzoglou I, Glielmi C, Sen A, Edelman RR. Prospective self-gated nonenhanced magnetic resonance angiography of the peripheral arteries. Magn Reson Med 2013;69:158–62.

27. Edelman RR, Giri S, Dunkle E, Galizia M, Amin P, Koktzoglou I. Quiescent-inflow single-shot magnetic resonance angiography using a highly undersampled radial k-space trajectory. Magn Reson Med 2013;70:1662–8.

28. Thierfelder KM, Meimarakis G, Nikolaou K, et al. Non-contrast-enhanced MR angiography at 3 Tesla in patients with advanced peripheral arterial occlusive disease. PLoS One 2014;9:e91078.

29. Koktzoglou I, Murphy IG, Giri S, Edelman RR. Quiescent interval low angle shot magnetic resonance angiography of the extracranial carotid arteries. Magn Reson Med 2016;75:2072–7.

30. Dietrich O, Raya JG, Reeder SB, Reiser MF, Schoenberg SO. Measurement of signal-to-noise ratios in MR images: influence of multichannel coils, parallel imaging, and reconstruction filters. J Magn Reson Imaging 2007;26:375–85.

31. American College of Radiology Committee on Drugs and Contrast Media. ACR Manual on Contrast Media. Available at: www.acr.org/~/media/37D84428BF1D4E1B9A3A2918DA9E27A3.pdf. Accessed February 15, 2016.

KEY WORDS cardiovascular magnetic resonance, noncontrast magnetic resonance angiography, quiescent interval single shot